DOI: 10.1002/chem.201103253

Highly Concentrated Aqueous Dispersions of Graphene Exfoliated by Sodium Taurodeoxycholate: Dispersion Behavior and Potential Application as a Catalyst Support for the Oxygen-Reduction Reaction

Zhenyu Sun,[a, b] Justus Masa,[c] Zhimin Liu,*[a] Wolfgang Schuhmann,[c] and Martin Muhler*[b]

Abstract: A high-yielding exfoliation of graphene at high concentrations in aqueous solutions is critical for both fundamental study and future applications. Herein, we demonstrate the formation of stable aqueous dispersions of pristine graphene by using the surfactant sodium taurodeoxycholate under tip sonication at concentrations of up to 7.1 mg mL^{-1}. TEM showed that about 8% of the graphene flakes consisted of monolayers and 82% of the flakes consisted of less than five layers. The dispersions were stable regardless of freezing (−20 °C) or heat treatment (80 °C) for 24 h. The concentration could be significantly improved to about 12 mg mL^{-1} by vacuum-evaporation of the dispersions at ambient temperature. The as-prepared graphene dispersions were readily cast into conductive films and were also processed to prepare Pt/graphene nanocomposites that were used as highly active electrocatalysts for the oxygen-reduction reaction.

Keywords: electrochemistry · exfoliation · graphene · oxygen · surfactants

Introduction

Producing processable graphene (G) sheets in large quantities remains an ongoing challenge for large-scale applications. To that end, pioneering work has been carried out through the aggressive oxidation of graphite, followed by exfoliation in aqueous or organic solvents to achieve graphene oxide (GO).[1] Subsequent chemical or thermal reduction is necessary to remove any epoxide, carboxy, or hydroxy groups, which complicates the processing. Whilst post-treatment can allow GO to partly regain its electrical conductivity, many defects in the sp^2 carbon lattice that were induced during the oxidation process cannot be fully reversed by reduction,[2] thus resulting in an undesirable degradation of the unique electronic properties of graphene.

To address these issues, a promising route is the exfoliation of pristine powdered graphite in the liquid phase to obtain graphene.[3–13] This top-down approach has an aesthetic appeal owing to its simplicity, straightforwardness, and its integration into various processes, such as impregnation, blending, casting, or functionalization; it utilizes low-cost and readily available graphite flakes and does not require transferring the graphene from the growth substrate. High-quality dispersions of graphene have been obtained by using such solvents, with Hansen solubility parameters that matched reasonably well with those suggested for graphene without oxidation or defect-formation.[3,8,12,13] Surfactant exfoliation is of particular interest as the solvent used is water. The mechanism for graphene-dispersion presumably involves hydrophilic and hydrophobic interactions, in which attraction between the graphene surface and the hydrophobic groups of the surfactants promotes adsorption, whilst the hydrophilic moieties associate with water.[10,11] The stabilization of dispersions in ionic surfactants results from the electrostatic repulsion between the ionic hydrophilic heads that coat adjacent graphene sheets.[10] For nonionic surfactants, steric hindrance contributes to the prevention of exfoliated graphene from re-aggregating. Despite recent advances in this field, graphene can only be dispersed at relatively low concentrations of the surfactants, typically no more than 0.3 mg mL^{-1}.[5,6,9–11] In addition, a high degree of exfoliation usually requires rather long-lasting bath sonication of up to 400 h in some cases.[9] Both aspects bring unfavorable limitations for many practical applications. Therefore, it is critical to consider new dispersing surfactants and also to develop efficient processes to enhance the maximum graphene con-

[a] Dr. Z. Sun, Prof. Dr. Z. Liu
Institute of Chemistry, Chinese Academy of Sciences
100190 Beijing (P.R. China)
E-mail: liuzm@iccas.ac.cn

[b] Dr. Z. Sun, Prof. Dr. M. Muhler
Laboratory of Industrial Chemistry
Ruhr-University Bochum
44780, Bochum (Germany)
E-mail: muhler@techem.rub.de

[c] J. Masa, Prof. Dr. W. Schuhmann
Analytische Chemie-Elektroanalytik & Sensorik
Ruhr-University Bochum
44780 Bochum (Germany)

Supporting information for this article, including characterization data and electrochemical measurements, is available on the WWW under http://dx.doi.org/10.1002/chem.201103253.

centration. On the other hand, although a number of surfactants have been used to disperse graphene, little research has been carried out to compare the dispersibility of graphene in different surfactants. In addition, optimal surfactant concentrations, at which the relative amount of graphene dispersed was maximized, have not been established.

Herein, we demonstrate such a surfactant and the processing procedure for the exfoliation of graphite to afford graphene in aqueous solutions. We show that by applying tip sonication for only 24 h, pristine graphene can be effectively exfoliated and stabilized in aqueous solutions of sodium taurodeoxycholate (STC) at very high concentrations of up to 7.1 mg mL^{-1}. A quantitative comparison of graphene dispersions in STC with the seven other commonly used surfactants, each at their optimum concentration, was conducted by using the absorbance per unit-cell-length at 660 nm. An extremely high concentration (12 mg mL^{-1}) was achieved by vacuum-evaporation of water from the graphene/STC dispersion under ambient temperatures. Finally, we show that these dispersions have promising applications in making conductive films and in preparing highly active graphene-based electrocatalysts.

Results and Discussion

An anionic surfactant with a high zeta potential (ζ), such as STC, was chosen for the exfoliation because the repulsive electrostatic potential barrier stabilizes the surfactant-coated graphene sheets against aggregation. The $|\zeta|$ of STC at its natural pH exceeds 60 mV, which may facilitate a high surfactant density on the graphene surfaces, thereby resulting in facile exfoliation and efficient stabilization of the dispersion. Previous work on graphene that was dispersed in *N*-methylpyrrolidone (NMP)[8] or sodium cholate (SC)[9] has demonstrated that the concentration of exfoliated graphene increased significantly with longer sonication times. Part of the reason for this has been hypothetically ascribed to the reduction of flake-size, which is controlled by the amount of sonic input energy. Alternatively, the input energy to the sample is also directly related to the sonication amplitude. In such a scenario, to optimize the processing procedure, we first investigated the dispersibility of graphene in STC as a function of sonication amplitude, and found a maximum value at 10% of the maximum output power (see the Supporting Information, Table S1). This value was surprising because we expected an enhancement of the dispersion concentration with increasing energy. One possible explanation for this phenomenon was that too-high a sonication power may have destroyed the aggregated structures of the surfactant that was adsorbed onto graphene, thereby leading to the degradation of its exfoliation level.

To find the optimum content of STC for graphene-exfoliation, the absorbance per unit-cell-length at 660 nm (A_{660}/l) was measured for a range of dispersions versus the STC concentration (at a fixed initial graphite concentration, $c_{G,i}$ = 5 mg mL^{-1}), which showed a surfactant concentration peak at 3 mg mL^{-1} (Figure 1). The STC concentration at which the dispersed graphene was maximized remained unchanged despite variation in the initial graphite concentration (Figure 2, top inset). As such, we chose to prepare all subsequent dispersions with c_{STC} = 3 mg mL^{-1}. The dispersibility of graphene in STC, in terms of A_{660}/l at their optimum concentrations, was twice as high as that in SC, which was recently reported to be one of the best-dispersing surfactants (Figure 1).[9] This result was attributed to the higher effective charge density on the head-group of STC and therefore to an increased repulsion between the graphene sheets. Furthermore, the dispersion behavior of graphene in seven other well-known surfactants was quantitatively studied in

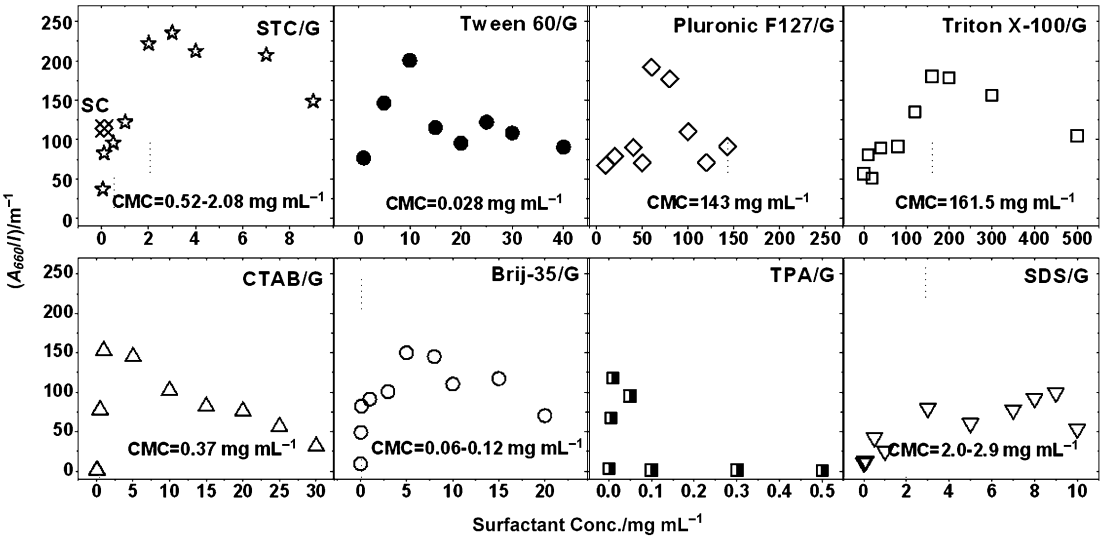

Figure 1. A_{660}/l, for the graphene dispersions (t_{sonic} = 5 h, centrifugation (CF): 5000 rpm for 90 min) as a function of surfactant concentration. The crossed-rhombus symbol in the top-left panel is a G/SC dispersion that was prepared under identical conditions at an optimum SC concentration of 0.1 mg mL^{-1}. The literature value (or range) of the CMC (mg L^{-1}) of each surfactant is shown in each panel (except for TPA, where it was unavailable).

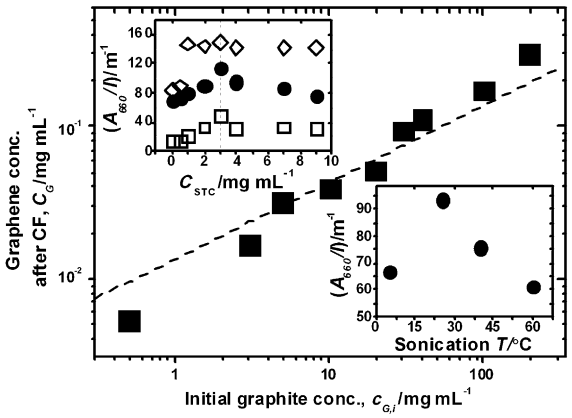

Figure 2. Concentration of graphene dispersion as a function of the starting graphite concentration. Upper inset: A_{660}/l versus c_{STC} for dispersions with $c_{G,i}=3$ (□), 10 (●), and 20 mg mL^{-1} (◇), respectively. Lower inset: A_{660}/l as a function of sonication temperature ($c_{G,i}=5$ mg mL^{-1}). In all cases: $t_{sonic}=45$ min, CF = 5000 rpm, 90 min.

terms of A_{660}/l as a function of surfactant concentration (Figure 1). The values of A_{660}/l for dispersions in Tween 60, Pluronic F127, and Triton X-100 were most-probably overestimated at high surfactant concentrations, owing to the corresponding increase in surfactant viscosity that led to more material being retained in the supernatant under fixed centrifugation parameters. The peaks for the majority of the surfactants occurred above their critical micelle concentration (CMC), which resembled carbon nanotube/surfactant dispersions.[14] The decrease in A_{660}/l at higher surfactant concentrations may have been due to attractive depletion interactions.[15] The discrepancy in the optimal surfactant concentration partly resulted from their various micelle hydrodynamic radii, and thus from their different effects on the extent of the depletion attraction.[16] By comparing A_{660}/l for the graphene dispersion in STC with seven other surfactants, each at their optimum concentrations, it was clear that STC had superior efficiency for dispersing graphene. Although non-ionic polymers Tween 60, Pluronic F127, and Triton X-100 also showed interesting dispersion capabilities for graphene, their large molecular weights, and thus highly viscous nature, imposed constraints on their further application. On the other hand, the optimum concentration of STC was reasonably low in comparison with the other surfactants. Another advantage of using STC for the exfoliation of graphene was its relative lack of toxicity, thus making it more user-friendly than traditional organic solvents and some surfactants. The extinction coefficient (α_G) was estimated to be 2920 mL mg^{-1} m^{-1} from the Beer–Lambert law ($A=\alpha_G c_G l$), where c_G was determined by TGA analysis (see the Supporting Information, Figure S2) together with the knowledge of the mass of graphitic material+STC after the evaporation of water for known volumes of dispersions; these values were in good agreement with those reported previously.[3,6]

Next, we considered the effect of sonication temperature (T_{sonic}) on the dispersion. We found that the values of A_{660}/l for the dispersions increased with increasing T_{sonic} in the range 5–25 °C, followed by a decrease at $T_{sonic}>25$ °C. A possible reason for this is that the effect of temperature on the assembly of STC on graphene surfaces dominates at $T_{sonic}\leq 25$ °C; that is, higher T promotes better adsorption of STC onto graphene and thus more-dispersed objects. Only a slight change of input power ($t_{sonic}=45$ min, $E_{25°C}-E_{5°C}\approx -1.5$ kJ) occurred as the T_{sonic} was raised from 5 to 25 °C. However, the effect of temperature on cavitation played a key role at higher $T_{sonic}>25$ °C; that is, it was more difficult for the cavitation to collapse with a rise in temperature, thereby leading to a big reduction of input power ($t_{sonic}=45$ min, $E_{60°C}-E_{25°C}\approx -10$ kJ), and consequently lower levels of graphene exfoliation. Consequently, subsequent graphene-dispersions were performed at $T_{sonic}\approx 25$ °C.

Keeping c_{STC} constant at 3 mg mL^{-1}, c_G was measured as a function of $c_{G,i}$ (Figure 2). An empirical relationship of $c_G=0.0136\times(c_{G,i})^{1/2}$ was observed ($t_{sonic}=45$ min, CF: 5000 rpm, 90 min), even at very high $c_{G,i}$. c_G increased steadily with $c_{G,i}$ and reached 0.3 mg mL^{-1} at $c_{G,i}=200$ mg mL^{-1}, a value that was only achieved with SC at lower CF rate (1500 rpm) and over a long sonication time (400 h). Moreover, the dispersed concentrations after centrifugation for 90 min at rates of 2000 and 5000 rpm were plotted as a function of sonication time (t_{sonic}; Figure 3a). In both cases, the concentration increased steadily with t_{sonic}, and reached values of about 3.4 and 1.3 mg mL^{-1}, respectively. Surprisingly, the concentration after CF for 90 min at 500 rpm ($t_{sonic}=24$ h) was as high as 7.1 mg mL^{-1}, which was much higher than both the best surfactant (SC)[9] and the best organic solvent (NMP),[8] and even surpasses the best results for GO in organic solvents.[17] To our knowledge, this is the highest concentration of pristine graphene in surfactants to date, and compares favorably to that of GO in water ($c_{GO}\approx 7$ mg mL^{-1}). In fact, the sediment could be recycled to obtain a further yield of graphene. Although we have obtained a significant increase in concentration at $c_{G,i}=200$ mg mL^{-1}, the limit of what can be dispersed is unknown and a larger graphene concentration may be achieved with a higher starting graphite concentration. In addition, in sharp contrast to 400 h of bath sonication required for graphene in either NMP[8] or SC,[9] the processing period herein (24 h) was dramatically reduced.

The concentration after CF at various rates (ω) is shown in Figure 3b. As expected, a steady decrease was observed, from about 7.1 mg mL^{-1} at 500 rpm to about 0.6 mg mL^{-1} at 13 000 rpm. In addition, the c_G value scaled empirically with ω^{-1} at $\omega\geq 2000$, as reported for G/SC.[9] Nevertheless, c_G deviated from the behavior at low ω (500 rpm), the exact reason for which is unclear at present.

We also found that a significantly higher concentration, about 12 mg mL^{-1}, could be achieved by vacuum evaporation of the dispersion ($t_{sonic}=24$ h, $c_{G,i}=200$ mg mL^{-1}, CF = 5000 rpm, 90 min) at room temperature. This result greatly broadens the potential application of graphene dispersions. The stability of the G/STC system was evaluated by monitoring A_{660}/l as a function of sedimentation time (Figure 3b, inset). The profile exhibited an exponential decay and was

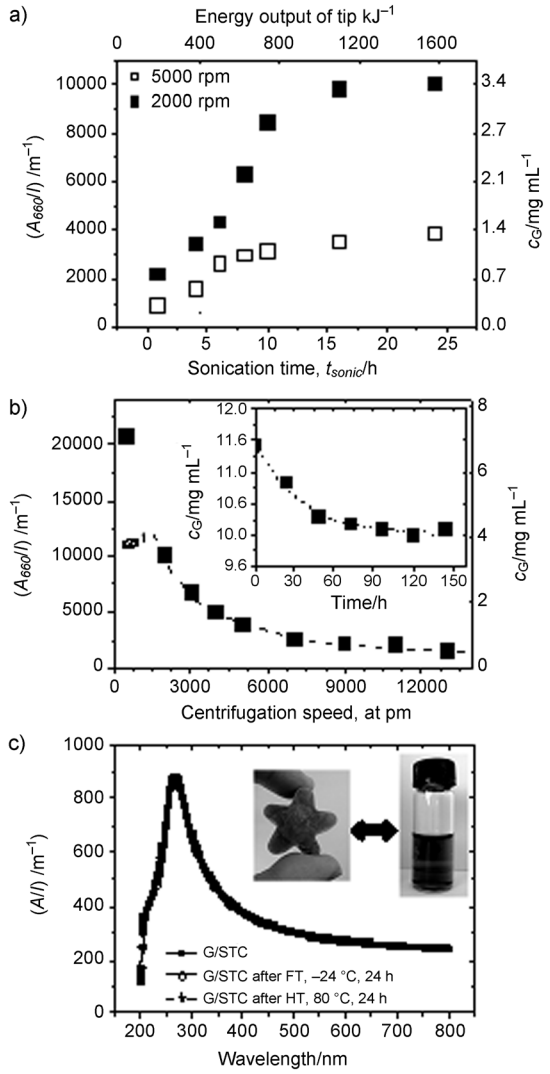

Figure 3. a) A_{660}/l versus t_{sonic} ($c_{G,i}=200$ mg mL^{-1}, CF = 90 min) for CF speeds of 2000 (■) and 5000 rpm (□). The upper axis shows the total energy output of the tip. b) A_{660}/l versus CF speed ($c_{G,i}=200$ mg mL^{-1}, $t_{sonic}=24$ h, CF = 90 min). Inset: A_{660}/l versus sedimentation time for the concentrated dispersion. c) Absorbance spectra before and after freezing (−20 °C) and heat treatment (80 °C) for 24 h. Inset: Photographs of the frozen and molten dispersions under ambient conditions. The Tyndall effect of the molten dispersion confirmed its colloidal nature. The right axis in (A) and (B) shows the graphite concentration calculated by using an absorption coefficient of 2920 mL mg^{-1} m^{-1}.

well-approximated by $c\ (t)=c_0+(c_T-c_0)\times e^{-t/\tau}$, where c_0 represents the concentration of the stable phase, c_T represents the initial concentration of the sedimenting material, and τ represents the sedimentation-time constant.[8,12,13] Fitting the data gave $c_0=10$ mg mL^{-1}, and $\tau=35$ h, which indicated that approximately 85% of the graphene in the concentrated dispersion remained stably dispersed against sedimentation over a reasonable long time. Small time constants suggested that the sedimenting flakes were relatively large. Moreover, no degradation of the dispersion occurred, even after freezing (−20 °C) or heating (80 °C) for 24 h, which was reflected by the maintenance of its absorption spectra after subjection to either treatment (Figure 3c). The strong peak at about 267 nm arose from the π-plasmon resonance that is commonly observed in graphitic materials,[11] whilst the absorption spectrum was featureless up to the visible range (800 nm), with a steady decrease in absorbance with increasing wavelength.[3,11]

Figure 4a and the Supporting Information, Figure S3 show representative TEM images of a large number of graphene flakes that were deposited onto a TEM grid; some folded sheets were also observed (marked by arrows). Figure 4b shows a TEM image of an individual thin flake with a high aspect ratio, Figure 4c shows a HRTEM image of a four-layer graphene sheet, and Figure 4d shows monolayer- and bilayer graphene sheets. Most of the observed flakes appeared to be of good quality with well-defined edges and free of holes or other damage. In addition to large sheets of up to several micrometers in length, flakes with dimensions of less than 100 nm were also discerned, primarily owing to sonication-induced cutting. By analyzing

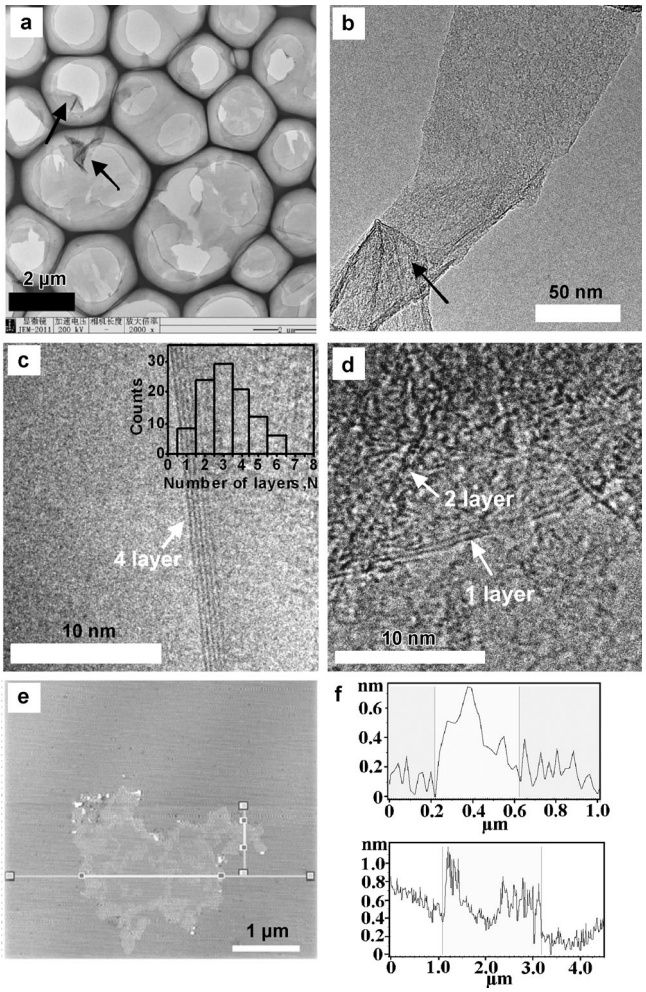

Figure 4. TEM images of a) large numbers of few-layer graphene flakes, and b) an individual graphene layer with possibly a folded sheet ($t_{sonic}=$ 24 h, CF = 5000 rpm, 90 min). HRTEM images of c) a four-layer, and d) monolayer and bilayer graphene sheets. e) AFM image of an individual graphene flake deposited onto mica. f) Profiles of line-scan height through the regions shown in (e).

the flake edges, we estimated the monolayer and few-layer (<5) number fractions to be about 8% and 82%, respectively, for a dispersion after CF at 500 rpm for 90 min. Atomic force microscopy (AFM) analysis observed a flake with a thickness of about 0.7 nm, which was consistent with monolayer graphene (Figure 4e).[18] The rugged topographic height profiles were probably due to the absorbed surfactant molecules on the graphene surface (Figure 4f).

X-ray photoelectron spectroscopy (XPS) analysis of the surface composition of a deposited graphene film revealed the presence of C (85.7 at.%), O (11.6 at.%), and S (0.4 at.%, the small amounts of S result from the residual surfactant in the film). The C 1s region was dominated by a peak at around 284.8 eV, which corresponded to graphitic carbon (Figure 5a). Deconvolution of the spectrum manifested two additional small peaks at 285.9 and 287.2 eV, which were assigned to C–O and C=O groups, respectively, thus indicating that a slight oxidation of graphite had occurred during the exfoliation process. The level of oxidation was small and the main C–C peak corresponded to about 86% of the spectrum, which was similar to G/SDBS as well as to the thermally annealed GO at 1100 °C in vacuum.[4,19] We expect that the degree of oxidation would be further decreased by introducing Ar (or N_2) to remove O_2 in the system during sonication.[20]

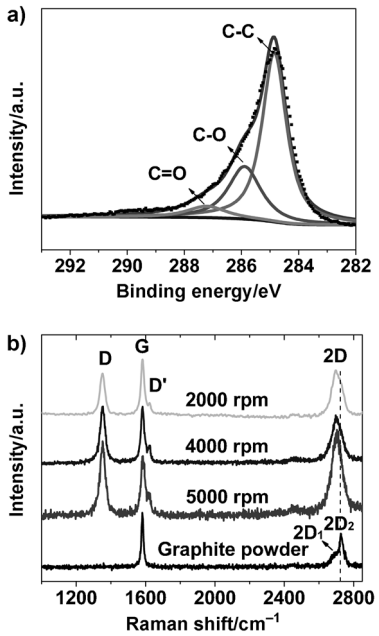

Figure 5. a) XPS pattern for a graphene film prepared by vacuum filtration. b) Raman spectra of the starting graphite powder for thin films that were prepared from dispersions (t_{sonic} = 24 h) with CF = 4000 and 2000 rpm, and for a sample that was prepared by drop-casting the dispersion onto silicon with CF = 5000 rpm (these spectra were normalized to the intensity of the G-band at 1582 cm^{-1}).

Raman spectroscopy enabled us to measure graphene thickness and to study any generated defects. The Raman spectra (Figure 5b) displayed three prominent peaks: a G band at about 1582 cm^{-1}, a second-order two-phonon-mode 2D (or G′) band at about 2700 cm^{-1}, and a disorder-related D peak at about 1351 cm^{-1}, as well as a weak D′ peak that appeared as a high-frequency shoulder to the G band. The G band is typically assigned to the first-order scattering of the E_{2g} mode of C sp^2 atoms, whilst the D band is associated with the breathing mode of κ-point phonons of A_{1g} symmetry. The 2D line with a single peak for the film samples is characteristic of thin flakes that are composed of less than 5 graphene layers that are positioned one on top of the other in a random orientation.[9,11,21] This result was in contrast with the doublet 2D shape for graphite, which consisted of two components ($2D_1$ and $2D_2$), which was indicative of an unperturbed ABAB stacking sequence along the *c*-direction of the bulk material.[21] A sharp and symmetric 2D band was observed for the drop-cast sample, thereby confirming the formation of single-layer graphene in STC,[21] whilst the peak was significantly broadened compared to that of monolayer graphene that was grown by chemical-vapor deposition, which may be due to the small size of the graphene produced herein.[21] The in-plane crystallite size of graphene was estimated to be approximately 53 nm at CF = 2000 rpm by $(2.4\times10^{-10})\lambda^4(I_D/I_G)^{-1}$, where λ is the laser energy in nanometers, and I_D and I_G are the intensities of the D and G modes, respectively.[22] Alternatively, a correlation of the D/G ratio and flake length by using $L\,nm^{-1}\approx260/(\Delta I_D/I_G)$ allowed us to estimate the flake length to be 350 nm.[12,13] This result agreed reasonably with TEM and SEM observations. The exfoliation of graphene was also supported by the observation that a shift (about 29 cm^{-1}) to lower wavenumbers occurred for the 2D band of graphene together with an enhancement of its intensity as compared to graphite.[20] Whilst the intensity of the D band relative to the G band (I_D/I_G) increased with CF rate, thereby indicating more defects for graphene sheets obtained with higher CF, the value of I_D/I_G with CF at rate of $\omega\leq2000$ rpm was less than 0.73. This result compared better with graphene sheets that were either produced from reduction of GO by hydrazine ($I_D/I_G\approx1.44$)[17] or by sodium-hydride reduction ($I_D/I_G\approx1.08$).[23] The defect population may be dominated by edge defects from small graphene flakes at rate $\omega\leq2000$ rpm, whilst the defects associated with vacancies and grain boundaries were also likely to be induced during intense sonication.[9,11]

Surfactant-stabilized graphene dispersions can be used in a range of applications, including the formation of films. SEM of a typical film showed that the flakes lay flat on top of each other, and many of the flakes were small, with diameters of 100–300 nm (Figure 6a). The edge of the film showed a well-defined layered morphology (Figure 6b). The as-shown film had a thickness of about 8 μm and a mean conductivity of about 13000 $S\,m^{-1}$ after annealing at 600 °C for 2 h under an Ar/H_2 atmosphere. This value was comparable to that of graphene films that were prepared from NMP dispersions[3] and compared favorably with reduced GO films that had been annealed.[24]

High-concentration graphene dispersions also elegantly offer the possibility of using a mild solvent-based approach

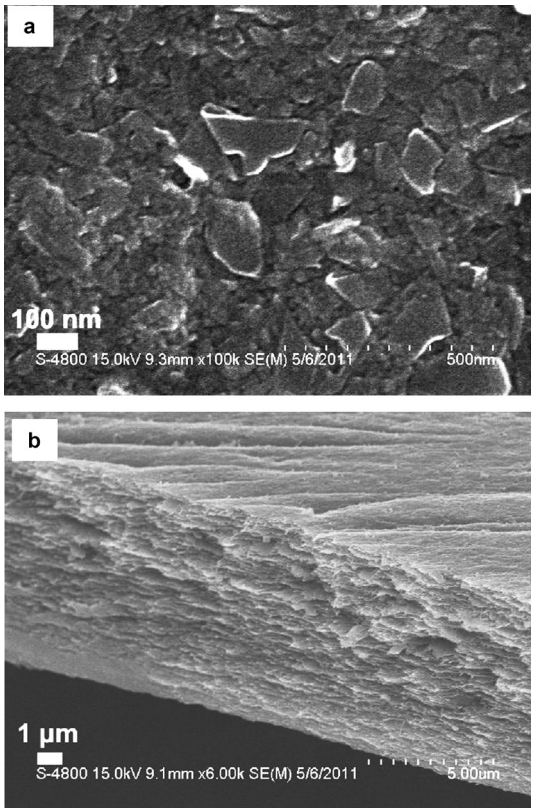

Figure 6. SEM images of a) the surface and b) the edge of a graphene film that was prepared from a dispersion after CF = 2000 rpm for 90 min.

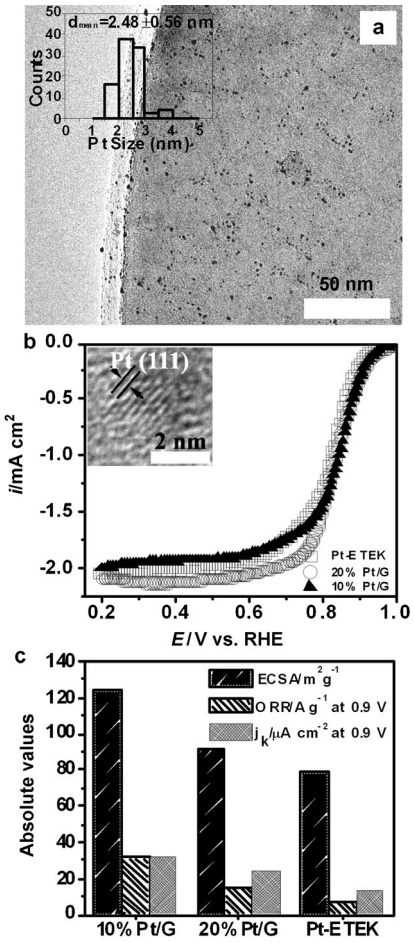

Figure 7. a) TEM image of 10% Pt/G. Inset: Size-distribution histogram of Pt NPs. b) Linear-sweep voltammograms for 10% Pt/G, 20% Pt/G ,and Pt-ETEK in an O_2-saturated 0.1 M $HClO_4$ solution (5 mV s^{-1}, rotation speed: 400 rpm). Inset: HRTEM of a Pt NP that was deposited onto G. c) Electrochemical surface area (ECSA), specific activity, and mass activity at 0.9 V for these three catalysts.

to design new G-based nanocomposites. Although recent reports have shown the decoration of metal nanoparticles (NPs) on GO or on reduced GO,[25–27] it remains an underexplored area of research and the creation of heterostructures of pristine graphene with unique intrinsic electrical properties is highly desirable. Herein, we demonstrate that Pt NPs with a quasi-uniform size and narrow size-distribution were deposited onto the surface of graphene by employing a sonication-facilitated decoration method (Figure 7a).[28] The mean size (diameter) of Pt NPs, as determined by directly measuring 100 particles by TEM analysis, was estimated to be approximately 2.48(±0.56) nm (Figure 7a, inset). HRTEM measurements (Figure 7b, inset) indicated the high crystallinity of the NPs, with an interplanar spacing of 0.23 nm, which corresponded to the {111} facet of Pt^0.[28] We performed RDE voltammograms to investigate the electrocatalytic activities of Pt/G with respect to the oxygen-reduction reaction (ORR) in acidic electrolyte. Exceptionally high electrochemically active surface areas (ECSAs; for the calculations, see the Supporting Information) were found for Pt/G (up to 91.8 and 123.8 $m^2 g^{-1}$ at 20% and 10% Pt loading, respectively), in contrast to Pt-ETEK (79.0 $m^2 g^{-1}$; 20% Pt on Vulcan carbon). To the best of our knowledge, this is one of the highest values reported to date and was most likely a result of the high dispersion of Pt NPs onto graphene sheets with a large surface area. On the other hand, graphene that was support with high electrical conductivity allowed an effective electron-transfer between the catalyst and the electrode surface. Significantly, the onset potential of the ORR for Pt/G at both 10 and 20% metal-loading was higher than that for the Pt-ETEK catalyst by at least 20 mV (Figure 7b). In addition, both the specific and mass activities (for the calculations, see the Supporting Information) of Pt/G catalysts were superior to those of Pt-ETEK (Figure 7c). These results suggested that graphene has promising applications as a competitive support in electrocatalysis. Studies are now underway with regard to a full mechanistic understanding of its activity.

Conclusion

We have produced stable aqueous dispersions of graphene through an efficient tip-sonication process by using the surfactant sodium taurodeoxycholate. The surfactant showed the highest dispersion ability for graphene reported to date.

The dispersed concentration increased with the initial graphite concentration and reached an unprecedentedly high concentration of up to 7.1 mg mL^{-1}. Vacuum evaporation of the dispersion gave a significantly improvement of the concentration (up to 12 mg mL^{-1}), 85% of which was stable over a long time. The dispersions have potential applications in conductive films and in highly efficient graphene-based electrocatalysts.

Experimental Section

Materials: Graphite powder was purchased from Sigma–Aldrich (product number 332461) and used as received. Anionic surfactants sodium taurodeoxycholate (STC), sodium cholate (SC), and sodium dodecylsulfate (SDS), cationic surfactants cetyltrimethylammoniumbromide (CTAB) and tetrasodium 1,3,6,8-pyrenetetrasulfonic acid (TPA), and nonionic surfactants Tween 60, Pluronic F-127, Triton X-100, and Brij 35 were purchased from Sigma–Aldrich and used as received. The structures of these surfactants are shown in the Supporting Information, Figure S1.

Surfactant-exfoliation of graphene: Stock surfactant solutions were prepared at the required concentration in Millipore water by stirring overnight. Herein, concentration is defined as the mass of solute/dispersed phase per volume of solvent. Graphene dispersions were prepared by adding graphite at various initial concentrations to solutions of surfactant (80 mL) in a 100 mL beaker. Various surfactant concentrations were explored. Ultrasonication was carried out by using a tip sonicator (Bandelin Sonoplus HD3100, 100 W, 20 kHz, 13 mm-diameter tip). To maintain sonication efficiency and to prevent overheating, the beaker was kept in an ice-water bath. Samples were pipetted from the beaker and left to stand overnight to allow any unstable graphite aggregates to form and then centrifuged for 90 min (Milipore-amicon MC-13). After centrifugation (CF), the top two-thirds of the dispersion were gently extracted by pipette.

Preparation of thin films: Thin films were prepared by vacuum filtration onto porous alumina membranes (Millipore, pore size 0.02 μm, membrane diameter 47 mm) and drying in a 60 °C oven.

Synthesis of Pt/G: In a typical procedure, a dispersion of G/STC (20 mL, t_{sonic} = 24 h, CF = 5000 rpm for 90 min) was first subjected to tip sonication for 2 min (30% of output amplitude), followed by the dropwise addition of $H_2PtCl_6{\cdot}6H_2O$ and an aqueous solution of $NaBH_4$ ($c_{NaBH_4} = 5c_{H_2PtCl_6{\cdot}6H_2O}$ (c is concentration), respectively, within 2 min sonication in either case.[29] All synthetic procedures were conducted under ambient conditions. The obtained mixture was centrifuged, and the collected precipitate was washed repeatedly with EtOH and subsequently with distilled water. Afterwards, the precipitate was re-dispersed in an EtOH bath and heated to reflux for 6 h to remove any remaining STC. Then, the obtained sample was vacuum-dried at 60 °C for 6 h.

Acknowledgements

We acknowledge financial support from the National Natural Science Foundation of China (No. 20903105).

[1] S. Stankovich, D. A. Dikin, G. H. B. Dommett, K. M. Kohlhaas, E. J. Zimney, E. A. Stach, R. D. Piner, S. T. Nguyen, R. S. Ruoff, *Nature* **2006**, *442*, 282–286.
[2] S. Stankovich, D. A. Dikin, R. D. Piner, K. A. Kohlhaas, A. Kleinhammes, Y. Jia, Y. Wu, S. T. Nguyen, R. S. Ruoff, *Carbon* **2007**, *45*, 1558–1565.
[3] Y. Hernandez, V. Nicolosi, M. Lotya, F. M. Blighe, Z. Y. Sun, S. De, I. T. McGovern, B. Holland, M. Byrne, Y. K. Gun'ko, J. J. Boland, P. Niraj, G. Duesberg, S. Krishnamurthy, R. Goodhue, J. Hutchison, V. Scardaci, A. C. Ferrari, J. N. Coleman, *Nat. Nanotechnol.* **2008**, *3*, 563–568.
[4] C. E. Hamilton, J. R. Lomeda, Z. Z. Sun, J. M. Tour, A. R. Barron, *Nano Lett.* **2009**, *9*, 3460–3462.
[5] M. Lotya, Y. Hernandez, P. J. King, R. J. Smith, V. Nicolosi, L. S. Karlsson, F. M. Blighe, S. De, Z. M. Wang, I. T. McGovern, G. S. Duesberg, J. N. Coleman, *J. Am. Chem. Soc.* **2009**, *131*, 3611–3620.
[6] A. A. Green, M. C. Hersam, *Nano Lett.* **2009**, *9*, 4031–4036.
[7] M. Zhang, R. R. Parajuli, D. Mastrogiovanni, B. Dai, P. Lo, W. Cheung, R. Brukh, P. L. Chiu, T. Zhou, Z. F. Liu, E. Garfunkel, H. X. He, *Small* **2010**, *6*, 1100–1107.
[8] U. Khan, A. O'Neill, M. Lotya, S. De, J. N. Coleman, *Small* **2010**, *6*, 864–871.
[9] M. Lotya, P. J. King, U. Khan, S. De, J. N. Coleman, *ACS Nano* **2010**, *4*, 3155–3162.
[10] R. J. Smith, M. Lotya, J. N. Coleman, *New J. Phys.* **2010**, *12*, 125008.
[11] J. T. Seo, A. A. Green, A. L. Antaris, M. C. Hersam, *J. Phys. Chem. Lett.* **2011**, *2*, 1004–1008.
[12] A. O'Neill, U. Khan, P. N. Nirmalraj, J. Boland, J. N. Coleman, *J. Phys. Chem. C* **2011**, *115*, 5422–5428.
[13] U. Khan, H. Porwal, A. O'Neill, K. Nawaz, P. May, J. N. Coleman, *Langmuir* **2011**, *27*, 9077–9082.
[14] Z. Y. Sun, V. Nicolosi, D. Rickard, S. D. Bergin, D. Aherne, J. N. Coleman, *J. Phys. Chem. C* **2008**, *112*, 10692–10699.
[15] B. Vigolo, A. Penicaud, C. Coulon, C. Sauder, R. Pailler, C. Journet, P. Bernier, P. Poulin, *Science* **2000**, *290*, 1331–1334.
[16] A. J. Blanch, C. E. Lenehan, J. S. Quinton, *J. Phys. Chem. B* **2010**, *114*, 9805–9811.
[17] V. C. Tung, M. J. Allen, Y. Yang, R. B. Kaner, *Nat. Nanotechnol.* **2009**, *4*, 25–29.
[18] X. H. An, T. Simmons, R. Shah, C. Wolfe, K. M. Lewis, M. Washington, S. K. Nayak, S. Talapatra, S. Kar, *Nano Lett.* **2010**, *10*, 4295–4301.
[19] H. A. Becerril, J. Mao, Z. Liu, R. M. Stoltenberg, Z. Bao, Y. Chen, *ACS Nano* **2008**, *2*, 463–470.
[20] H. X. Xu, K. S. Suslick, *J. Am. Chem. Soc.* **2011**, *133*, 9148–9151.
[21] A. C. Ferrari, J. C. Meyer, V. Scardaci, C. Casiraghi, M. Lazzeri, F. Mauri, S. Piscanec, D. Jiang, K. S. Novoselov, S. Roth, A. K. Geim, *Phys. Rev. Lett.* **2006**, *97*, 187401.
[22] M. H. Rummeli, A. Bachmatiuk, A. Scott, F. Borrnert, J. H. Warner, V. Hoffman, J. H. Lin, G. Cuniberti, B. Buchner, *ACS Nano* **2010**, *4*, 4206–4210.
[23] N. Mohanty, A. Nagaraja, J. Armesto, V. Berry, *Small* **2010**, *6*, 226–231.
[24] H. Chen, M. B. Muller, K. J. Gilmore, G. G. Wallace, D. Li, *Adv. Mater.* **2008**, *20*, 3557–3561.
[25] S. J. Guo, D. Wen, Y. M. Zhai, S. J. Dong, E. K. Wang, *ACS Nano* **2010**, *4*, 3959–3968.
[26] P. V. Kamat, *J. Phys. Chem. Lett.* **2010**, *1*, 520–527.
[27] Z. Jin, D. Nackashi, W. Lu, C. Kittrell, J. M. Tour, *Chem. Mater.* **2010**, *22*, 5695–5699.
[28] Z. Y. Sun, Y. F. Zhao, Y. Xie, R. T. Tao, H. Y. Zhang, C. L. Huang, Z. M. Liu, *Green Chem.* **2010**, *12*, 1007–1011.
[29] Z. Y. Sun, X. Wang, Z. M. Liu, H. Y. Zhang, P. Yu, L. Q. Mao, *Langmuir* **2010**, *26*, 12383–12389.

Received: October 14, 2011
Revised: January 20, 2012
Published online: ■■ ■■, 0000

Graphene

*Z. Sun, J. Masa, Z. Liu,**
*W. Schuhmann, M. Muhler** ■■■■–■■■■

Highly Concentrated Aqueous Dispersions of Graphene Exfoliated by Sodium Taurodeoxycholate: Dispersion Behavior and Potential Application as a Catalyst Support for the Oxygen-Reduction Reaction

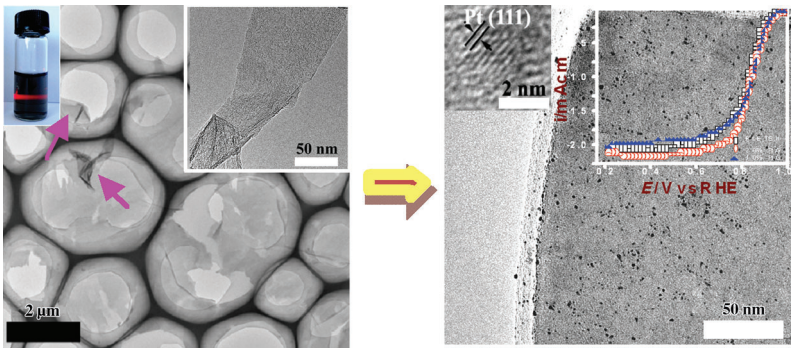

The great dispersion: Stable aqueous dispersions of pristine graphene were achieved by using the superior surfactant sodium taurodeoxycholate with the aid of tip sonication at very high concentrations (up to 7.1 mg mL^{-1}). The dispersions have potential applications in conductive films and in highly active electrocatalysts (see figure).